Research Article

Iftikhar Abdulsahib, Miami M. Hilal*, Mohammed Y. Fattah and Anmar Dulaimi

Performance evaluation of grouted porous asphalt concrete

https://doi.org/10.1515/eng-2022-0556
received September 15, 2023; accepted November 06, 2023

Abstract: Semiflexible pavement (SFP) is considered a composite mixture, as it consists mainly of a porous asphalt mixture with high air voids grouted with highly flowed cementitious grout. Numerous benefits have been attributed to this technology, including exceptional slip resistance, a high static bearing capacity, and rutting resistance. In this study, two different types of semiflexible paving mix were produced by using two different types of grouting materials (GMs). There is a discrepancy between the compressive strengths of the two GMs used, as the compressive strength of the first mixture, which consisted of 96% cement and 4% silica fume (SF), was approximately twice the compressive strength of the second mixture, which consisted of 75% cement and 25% sand. The mechanical and durable properties of the two SFPs were studied, in addition to the effect of variation in the compressive strengths of the two GMs and their effect on the final performance of the pavement. The results of Marshall and rutting tests show that the SFP material exhibits good high-temperature stability. The effect of the variation in the compressive strength of the two mixtures was evident in the results of the tests compared with the sand mixture at a strength of 20.8 MPa, the SF at a strength of 48.1 MPa witnessed a 39.54% increase in the Marshall stability at 28-day curing age. Also, the composite material (CM) showed better rutting performance than traditional asphalt mixtures, which did not exceed 2 mm. The results of the indirect tensile strength (ITS) test showed a discrepancy between the two types of CM, as the ITS value of the grouting material of SF (GMSF) mixture increased by 14.91% compared with the grouting material of sand (GMSN) for the curing age of 28 days for unconditioned samples and by 20.22% for the conditioned samples for the same curing age, while the durability of two types of CM was measured by Cantabro abrasion loss and tensile strength ratio. The results were acceptable and within the specification limits. With a variation for the two types of CM, the GMSF mixture showed an increase in the value of Cantabro loss by 11.52% over the GMSN mixture for ageing samples and 6.59% for non-aging samples of 28 days of curing age.

Keywords: SFP, composite material, grouting, performance, silica fume

1 Introduction

Semiflexible pavements (SFPs) are a variety of high-performance pavements that were developed in France in the 1950s and were initially used to pave runways at airports, which exhibited excellent road performance [1]. Subsequently, Britain, the United States, the former Soviet Union, and other nations conducted research on SFP, demonstrating that the pavement material can extend the pavement's service life and has excellent high-temperature stability [2]. SFP comprises a porous asphalt mixture (PAM) mattress with a void rate in the range of 20–35%, grouted with high-fluidity cement mortar (HCM) [3,4]. The enhanced performance of cement grouting asphalt macadam materials, also known as SFP materials, in contrast to conventional asphalt concrete materials, may be attributed to the inclusion of cement grouting material (GM) and matrix asphalt mixture [5]. It features the flexibility of asphalt pavement and the rigidity of rigid pavement in different degrees and has been widely used in many countries [6,7]. Numerous benefits have been attributed to this technology, including exceptional slip resistance, good oil resistance and colourability, high static bearing capacity, and rutting resistance. In addition, its viscoelastic behaviour can increase load tolerance without causing ruts, reduce the number of temperature joints, or even eliminate the need for a setting, thereby enhancing driving comfort [8,9]. SFP provides a viable option for bridge

*** Corresponding author: Miami M. Hilal,** Civil Engineering Department, University of Technology-Iraq, Baghdad, Iraq, e-mail: 40092@uotechnology.edu.iq
Iftikhar Abdulsahib: Civil Engineering Department, University of Technology-Iraq, Baghdad, Iraq, e-mail: abce.21.39@grad.uotechnology.edu.iq
Mohammed Y. Fattah: Civil Engineering Department, University of Technology-Iraq, Baghdad, Iraq, e-mail: 40011@uotechnology.edu.iq
Anmar Dulaimi: College of Engineering, University of Warith Al-Anbiyaa, Karbala 56001, Iraq, e-mail: a.f.dulaimi@uowa.edu.iq

deck overlay because it outperforms traditional hot-mix asphalt pavements in terms of longevity and strength [10]; SFP construction is typically a two-phase process. First, the PAM mattress is prepared and paved with lighter or comparable equipment to that used for traditional asphalt concrete. After the asphalt has chilled, the surface can be coated with HCM. Due to the excellent connectivity of voids in the PAM, HCM penetrates the entire layer with rubber scrapers and light vibrating rollers to obtain a very low residential void rate for SFP. After a few days of curing, the SFP eventually attains the required traffic strength.

Hou et al. [11] evaluated the mechanical properties and durability of SFP materials and demonstrated that they exhibit superior high-temperature stability, fatigue performance, and water stability compared to conventional asphalt mixtures. Yang [5] assessed the performance of SFPs by analysing the volumetric parameters of the matrix asphalt mixtures. The findings revealed that the SFP materials exhibited superior high-temperature stability and low-temperature stability compared to conventional asphalt pavement materials. The formation of SFP materials from asphalt concrete skeletons under five distinct gradation types was investigated by Zhao and Yang [12], and the low-temperature fracture resistance performance of these five skeletons was evaluated. The results demonstrated that the low-temperature fracture resistance capability of SFP materials based on continuously graded asphalt concrete skeletons was superior to that of other SFP materials. Comparing SFP and conventional bituminous mixtures has revealed that at higher temperatures, the ITS values of SFP exhibit an increase of 2–3 times compared to bituminous concrete mixtures [10,13]. Hao et al. [14] examined differences between the SFP and dense-graded asphalt mixtures and highlighted SFP's superior performance at low temperatures and increased resistance to moisture damage, while Zhao et al. [15] conducted an investigation and discovered an improvement in the ability of semiflexible materials to resist cracking at low temperatures after modifying the asphalt within the hot mix asphalt (HMA) structure.

A study conducted by Hassan et al. examined the impact of fly ash and silica fume (SF) on the performance of cement mortar in relation to the GM. The researchers concluded that the incorporation of fly ash and silicon has the potential to enhance both the workability and mechanical properties of cement mortar used for SFP [16]. The performance of the pavement, including stone matrix asphalt, is influenced by the bond strength between the cement and asphalt interface subsequent to the pouring of cement grout into the asphalt mixture. Inadequate contact at the interface leads to insufficient mechanical strength and suboptimal deformation characteristics. Zhou analysed the failure mode of SFP, highlighting that the typical damage in this type of pavement primarily manifests at the interface between cement and asphalt, as well as within the cement material itself. [17]. Yang [5] found that the cement slurry infusion can significantly improve the compressive strength of the material and contribute to even better mechanical properties when the GM strength is 40.2 MPa.

Nevertheless, the research failed to examine the precise characteristics of viscosity and elasticity in the skeleton of HMA that offer greater benefits in enhancing the resistance to low-temperature cracking in semiflexible materials. The cost of semiflexible anti-rutting pavement was approximately 1.5–2 times more than that of conventional asphalt pavement. Despite the relatively larger initial expenditure, the longevity of the service life for the alternative asphalt pavement was found to be tenfold more than that of conventional asphalt pavement. The implementation of this solution has the potential to substantially decrease yearly maintenance duration and expenses, alleviate traffic congestion, and generate notable economic and social advantages [18].

The objective of this study is to assess the engineering properties of an SFP. As a way to investigate the influence of compressive strength on the ultimate performance of SFP, two distinct GMs possessing varying compressive strengths were employed; the experimental procedure commenced by formulating a PAM characterized by an air void ratio within the range of 25–35%. Subsequently, the mixture was subjected to grouting using two distinct GMs, each possessing varying levels of compressive strength. The initial mixture had a compressive strength of 48.1 MPa, while the subsequent mixture demonstrated a compressive strength of 20.8 MPa. Upon completion of the necessary sample preparations, the performance evaluation of the samples was subjected to several laboratory tests. These tests included the assessment of Marshall stability, the indirect tensile strength (ITS), the compressive strength, the wheel truck test, the Cantapro loss test, and tensile strength ratio.

2 Materials

Raw materials used in this study include asphalt, aggregate, cement, SF, sand, and superplasticizer (SP) with poly-carboxylate.

2.1 Asphalt cement

The production of the PAM involved the utilization of SBS-modified asphalt cement. The utilization of styrene–butadiene–styrene (SBS) has resulted in enhancements to the

Table 1: Physical and mechanical properties of SBS

Property or characteristics	Unit	Requirement
Density	kg/m^3	940
Tensile strength (σt)	MPa	32 min
Melting point	°C	180
Elongation	%	88

asphalt cement with a 40/50 grade. The incorporation of a poly-butadiene block imparts elasticity, while the addition of a polystyrene block confers plastic properties to the asphalt mixture. This enhancement in performance is achieved through the augmentation of stiffness, stability, and elasticity of the asphalt binder. The asphalt binder was supplemented with SBS at a concentration of 4% relative to the weight of the asphalt. Tables 1 and 2 present the physical and mechanical characteristics of SBS and modified asphalt materials.

2.2 Aggregate

The present study utilizes a regional aggregate comprising crushed quartz sourced from the Al-Nibaie quarry, which is extensively employed in Iraq's asphalt mixing facilities. The coarse and fine aggregates utilized in the study underwent a process of washing, sieving, and subsequent recombination to achieve the appropriate proportions, as specified by the SCRB (SCRB/R9, 2003) [10] for the wearing course gradations. Table 3 presents the physical characteristics of both fine and coarse aggregates.

2.3 Cement

The cement used in this study is ordinary Portland cement (OPC), specifically CEM I 42.5N-SR 3.5, which adheres to the Iraqi specification No.5/1984 type I [19]. Table 4 presents a comprehensive overview of the chemical and physical parameters associated with this particular variant of cement.

Table 2: Physical properties of asphalt modified with 4% SBS

Test	Unit	Specification	Result
Penetration (25°C–100 g–5 s)	1/10 mm	ASTM D5	35
Ductility (25°C, 5 cm/min)	cm	ASTM D113	140
Flash point (cleave land open cup)	°C	ASTM D92	326
Fire point	°C	ASTM D92	368
Softening point	°C	ASTM D36	72
Solubility in trichloroethylene	%	ASTM D2042-01	99.3
**RV 135°C	Pa·s	ASTM D4402	1.35
**RV 165°C			0.75
After thin-film oven test (ASTM D1754)			
Retained penetration; % of original	%	ASTM D5	80
Ductility of residue (25°C–5 cm/min)	cm	ASTM D113	110

**Rotational viscometer.

2.4 SF

The incorporation of fine-grained supplementary cementitious materials, such as SF, into the composite cement paste has been found to decrease the interparticle porosity of cement and improve the impermeability, flexural strength, and compressive strength of the GM. Table 5 presents the characteristics of the SF utilized in the investigation.

2.5 SP material

SP was used in the liquid form, as it was found to disperse faster during mixing and thus increase workability. It also

Table 3: Physical properties of aggregates

Property	Specification	Coarse aggregate	Fine aggregate
Bulk specific gravity	ASTM C127-128-15	2.611	2.658
Apparent specific gravity	ASTM C127-128-15	2.662	2.733
% of absorption	ASTM C127-128-15	0.52	0.73
Los Angeles abrasion	ASTM C131-14	17.72	—
Percent flat and elongated particles, 10% max	ASTM D4791-10	5	—
Fractured pieces %	ASTM D5821-13	98	—
Clay content by sand equivalent% 45 min	ASTM D2419-14	—	51

Table 4: Physical and chemical properties of OPC

Property	Results	Iraqi Specification 1984 [19]
Physical properties		
Fineness (m^2/kg)	340	250
Density (g/cm^3)	2.1	2.981
Initial setting time (min) ≥45	149	(min) ≥ 45
Final setting time (h)	3.14	≤10
Expansion (mm)	1	≤10
Property	**Results**	**Requirement**
Chemical properties		
SiO_2	19.9	—
Al_2O_3	4.57	—
Fe_2O_3	4.82	—
CaO	61.11	—
MgO	3.13	≤5%
SO_3	2.234	C_3A ≤ 5% SO_3 ≤ 2.5% C_3A more than 5% SO_3 ≤ 2.8%
Na_2O_3	0.20	—
K_2O	0.52	—
Chloride	0.018	—
Loss of ignition LOI	2.92	≤4.0%
Eq. alkalis	0.53	<0.6% for low alkalis
*IR	1.08	≤1.5%
**LSF	0.9503	0.66–1.02%
C_3A	3.98	>3.5%

*Insoluble residue.
**Lime saturation factor.

conforms to the high-range water, reducing to EN 934-2 SP [20]. Table 6 illustrates the properties of SP used in the study.

2.6. Sand

The sand used in this study was brought from Al-Najaf city. Sand does not contain fine particles or gravel particles, and soil is classified, according to the Unified Soil Classification System, as poorly graded sand (SP). Figure 1 illustrates the particle size distribution curve for the adopted sand.

Table 5: Properties of SF used in the study

Property	Value	ASTM-C1240 2018
Color	Grey	—
Size	0.149	~0.15 μm
Specific surface area	16,500	≥15,000 cm^2/g
Specific gravity	2.1	—
Physical form	Powder	—
Bulk density	0.6	0.5 ± 0.1 kg/l
Moisture	0%	<2%

Table 6: Properties of the SP material

Property	Value	Specification (EN 934-2)
Form	Viscous liquid	—
pH	6.6	5.9-7.9
Relative density	1.06 ± 0.02	1.06–1.1 kg/l
Colour	Light brown	—
Viscosity	128 ± 30 cps	—

3 Experimental work

The laboratory work first began with the preparation of the PAM to achieve the required void ratio by determining the required aggregate gradation and the optimal bitumen content. The second stage required designing the GM to achieve the required fluidity and strength and then preparing SFP samples for laboratory evaluation of performance.

3.1 Preparation of the PAM

A PAM is utilized only as a coarse surface [21]. However, this type of pavement was used as a skeletal structure to contain the GM. The PAM was designed to achieve an air void ratio ranging between 25 and 35%, where a gradation of aggregates was chosen within the limits of the American specification [22], characterized by a high proportion of coarse aggregate to achieve the largest possible air void ratio, as shown in Table 7.

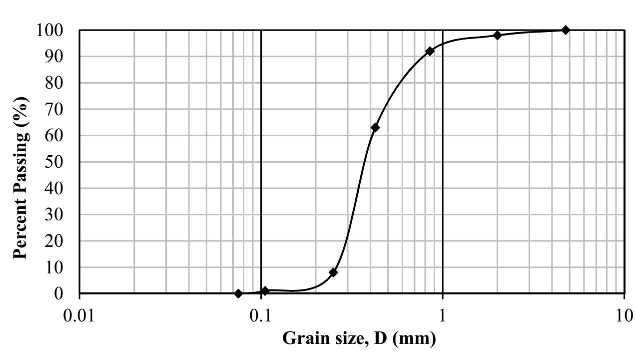

Figure 1: Gradation of sand used in the study.

Table 7: Aggregate gradation used in the study

Sieve size (mm)	ASTM D7064-13 % passing	Selected% passing
19	100	100
12.5	85–100	86
9.5	35–60	35.5
4.75	10–25	10.5
2.36	5–10	5
0.075	2–4	3

Then, the optimal bitumen ratio was determined based on the following equation [3]:

$$AC = 3.25 \times (\alpha) \times \Sigma^{0.2}, \quad (1)$$

$$\alpha = 2.65/\mathrm{SGagg}, \quad (2)$$

$$\Sigma = 0.21C + 5.4S + 7.2s + 135f, \quad (3)$$

where OBC is the optimum bitumen content, SGagg is the apparent specific gravity of the aggregate blend, Σ is the specific surface area, C is the percentage of material retained on a 4.75 mm sieve, S is the percentage of material passing through a 4.75 mm sieve and retained on a 600 µm sieve, s is the percentage of material passing through a 600 µm sieve and retained on a 75 µm sieve, and f is the percentage of material passing through a 75 µm sieve.

The percentage of bitumen reached 4.1% of the mixture weight. The determination of the appropriate number of blows or gyrations for compacting high void bituminous mixes now lacks sufficient criteria. Various compaction methods have been employed by researchers for these mixtures. Several researchers have employed different quantities of Marshall blows (ranging from 10 to 75), administered on either one or both surfaces [10,11,23,24], while others have used the gyratory compactor [16,25]. During this study, three levels of humping stress were tested to achieve the required void ratio (50, 35, 20) for each face. From the results obtained, it was found that the 35 blows on each face achieved the required void ratio, which amounted to 31.4% of the sample size.

3.2 GM design (fluidity and strength)

The laboratory tests that were conducted on the appropriate GM are summarized in two basic tests. The first is the fluidity test, which has been subject to the American standard C939-97 [26]. In this test, 1,500 ml of the grouting sample is passed through a cone with special dimensions. Figure 2 shows the shape and dimensions of the cone used in the test, and the time required for this quantity to run out from the cone is calculated by using a stopwatch in seconds, and ranges between (9–16) sec. [27].

The second test is the compressive strength test, which was subject to the specification [20]. As shown in Figure 3, to determine the hardness and resistance of the GM, the cubic samples were cast with dimensions of 5 cm × 5 cm × 5 cm and tested at three curing ages of 1, 7, and 28 days. Two GMs were used, the first consisting of cement, SF, and SP, which were used in different proportions with different water–cement ratios to obtain the optimal mixture for use as a GM. Figures 4 and 5 show the effect of w/c and % SP on the workability of the mixture.

As for the second mixture, cement and sand were used in different proportions, as well as the SP, to obtain the fluids required for the mixture, as shown in Figures 6 and 7.

The results showed an increase in workability with an increase in the ratio of water to cement in a direct phase, which is considered the main factor affecting the workability of mixtures with a noticeable effect of the SP on the workability.

Figure 2: Cone used in the flow cone test.

Figure 3: Compression machine.

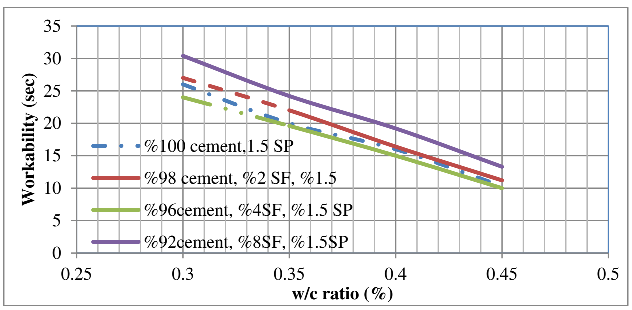

Figure 4: The effect of the w/c ratio on the SF mixture workability.

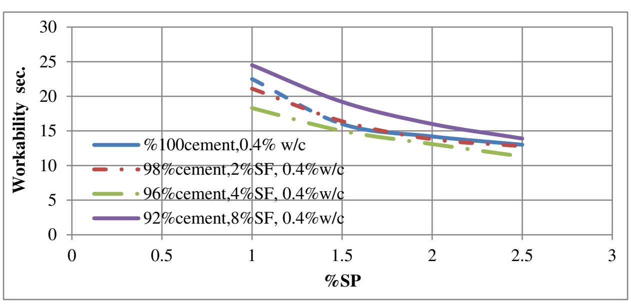

Figure 5: The effect of SP% on the SF mixture workability.

It is clear from Figure 5 that there is an increase in the percentage of SP material with the increase in the percentage of SF, and this is completely consistent with what has been observed [15]. This is due to the very fine size of particles of SF, which causes the absorption of some of the SPs on its surface. As for sand, its granules are considered large compared to SF granules. However, the percentage of SP increases with the increase in the percentage of sand. This is because an increase in the percentage of sand in the mixture leads to a significant decrease in the percentage of cement in it, and this, in turn, leads to a decrease in the value of SP used as a percentage of the weight of cement, and this leads to an increase in the percentage of SP to achieve the required liquidity. By the results of the fluidity test, the mixtures for which the compressive strength will be tested were determined, as the percentages (96% cement, 4% SF, 1.5% SP, 4% w/c) were determined for the SF mixture, as it gave the required compressive strength, which is not less than 40 MPa. As for the sand mixture, the results of the compressive strength test were less than the required limit for all proportions but in varying proportions, as 50% sand showed the highest strength, which amounted to 34.7, while 25% sand showed its lowest strength for 28 days. Figure 8 shows the development of the compressive strength of the selected mixtures with curing age.

4 Preparation of SFP specimens

Laboratory samples of porous material were prepared in two distinct forms, namely cylinder and slab specimens, in accordance with the specific requirements of the test procedure. The test samples were fabricated using identical materials and procedures in order to ensure consistency across all laboratory specimens. The production and

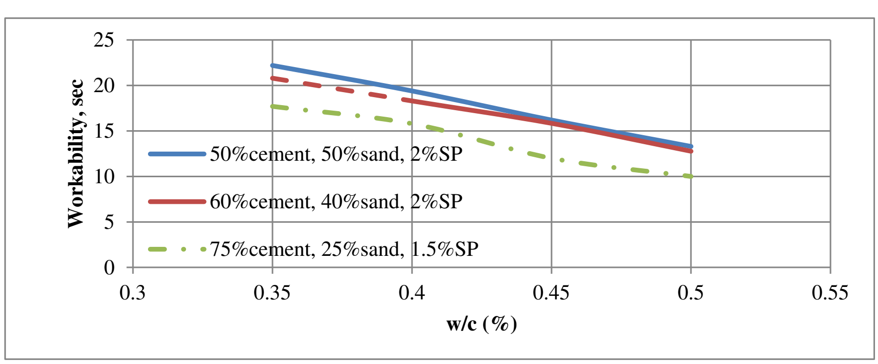

Figure 6: The effect of the w/c ratio on sand mixture workability.

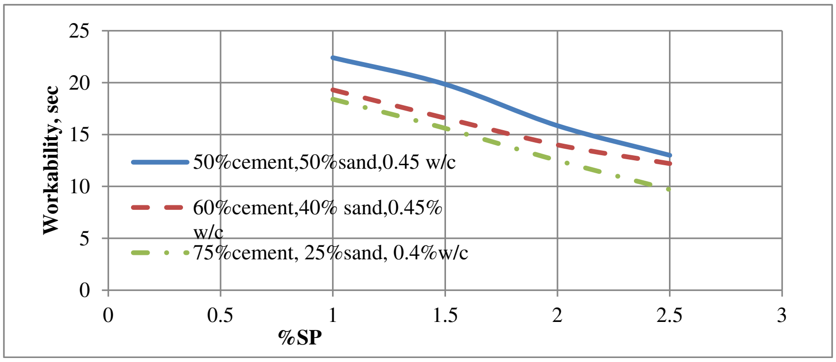

Figure 7: The effect of SP percentage on sand mixture workability.

curing processes were devised with the intention of closely emulating the circumstances experienced on the field. In order to achieve the desired void ratio for the final design, the PAM, consisting of a hot asphalt mix, was carefully deposited into a Marshall mould and subsequently compacted using 35 blows on each side. In a similar vein, the rectangular slab specimens of PAM employed in the wheel tracking test were manufactured within moulds with a slab compactor, with the aim of achieving a specific void ratio. The slab samples had dimensions of 40 cm in length, 30 cm in width, and 5 cm in thickness. Volumetric calculations were conducted to ascertain the optimal quantity of the hot asphalt mix necessary to achieve the desired void ratio in the final mixture by considering the size of the mould. The asphalt mix was placed in the mould, and an asphalt slab compactor device compacted the mix. The specimens were then air-cooled for a minimum of 4 h in order to prepare them for grouting. Then, the samples were wrapped with aluminium foil used for cooking, and then they were also wrapped with a layer of nylon for cooking as well. To ensure that the GM did not leak out, the cement slurry was added to PAM cylinder and slab samples using gravitational force. The grouting began first with the SF mixture, and a smooth penetration of the GM was observed, as shown in Figure 9.

The grouting of the sand mixture began at a rate of 50%. In the beginning, it was noticed that the sand granules accumulated on the surface of the sample, causing closure of the surface air spaces and thus preventing the GM from penetrating, so this percentage was excluded from the work. The percentage of sand was 25%, which showed good penetration into the layer. The reason for this may be due to the high percentage of sand in the mixture and the large size of the sand grains compared to the size of the cement grains, which caused the inhomogeneity of the two materials and the small path of the internal air voids need a high fluidity homogeneous material to penetrate.

5 Evaluation of the mechanical properties

This section provides a comprehensive overview of the mechanical strength tests conducted on samples manufactured in the laboratory.

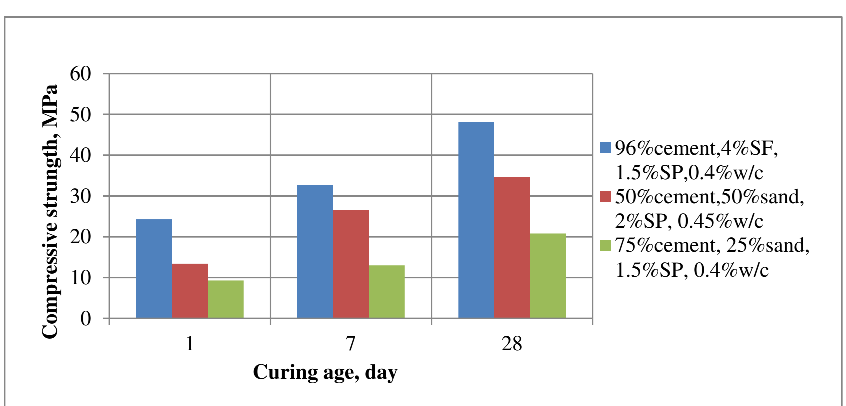

Figure 8: Improvement of the compressive strength with curing age for selected mixtures.

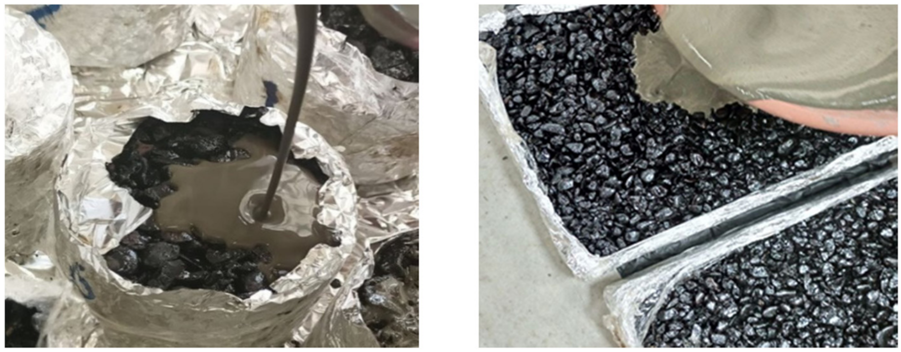

Figure 9: Grouting process of porous asphalt mixture samples.

Figure 10: Samples tested by the Marshall stability test.

5.1 Marshall tests

The SFP mixture's stability was assessed using the Marshall test according to ASTM D6927 [28], as shown in Figure 10. The results of Marshall stability and flow for two types of SFP with different curing times at 1, 7, and 28 days are shown in Figures 11 and 12, respectively. It is clear from the results that SFP has greater Marshall stability and lower flow value than those of traditional asphalt concrete due to its enhanced strength and fewer residual voids by grouting cement mortar, and this is consistent with the results of Hassan et al. [16], noting that the Marshall stability increases with increasing curing age of the GM. The maximum value of Marshall stability was achieved at 32.75 kN with 4% replacement of cement with SF at 28 days.

The influence of the compressive strength of GMs is evident in the stability value of the SFP, where the compressive strength value of the grouting mixture improved with 4% SF, which was nearly twice the value of the compressive strength of the 25% sand mixture. This is consistent with Yang [5]

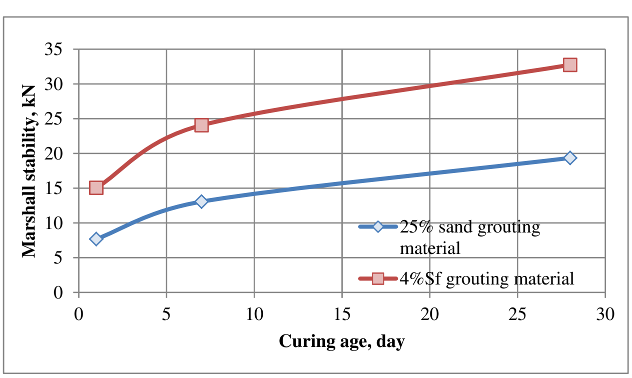

Figure 11: Marshall stability value for different curing ages of two types of SFP.

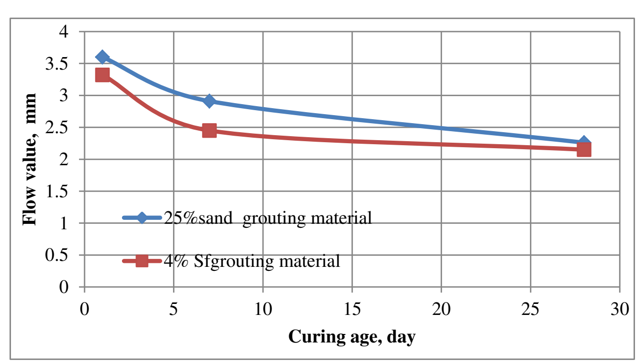

Figure 12: Flow value for different curing ages of two types of SFP.

results that Marshall stability increases with increasing the compressive strength of the GM.

During this study, the percentage of air voids after grouting was not calculated; X-ray CT scanning could be a good method to achieve this.

5.2 ITS

The determination of the ITS was conducted using the ASTM D6931 (2012) [29] standard. This involved subjecting cylindrical samples to loading along a diametrical axis. The specimen's maximum load, denoted as *P*, was utilized in the computation of the ITS. Figure 13 illustrates the outcomes of two distinct categories of SFP alongside three varying durations of curing, namely 1, 7, and 28 days. The result of ITS for conditioned samples at 28 days is shown in Figure 13. Generally, the ITS values increase with increasing curing time for all mixes. This can be attributed to the cement hydration reaction, which requires more time to complete, and the enhanced strength of mixes, as illustrated in Figure 14.

The results also show the difference between the ITS values for the two types of semiflexible paving used in this study, where the type resulting from the injection of cement and SF, which has the highest compressive strength, showed higher values than the type resulting from the injection of cement and sand, and this agrees with the results of Solouki [30]. This also agrees with the results of Momtaz et al. [31] achieved from the fracture shape of the ITS test; it was clear that there was no division of the mixture. Approximately, similar shapes of failure were noticed in all samples. The failure shape of the semiflexible samples was completely different from that of concrete specimens. This is a good indicator that the GA mix, or SFP, is still flexible.

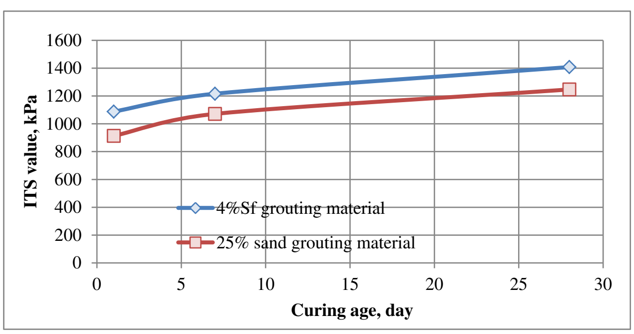

Figure 13: ITS values for two types of SFPs at different curing ages.

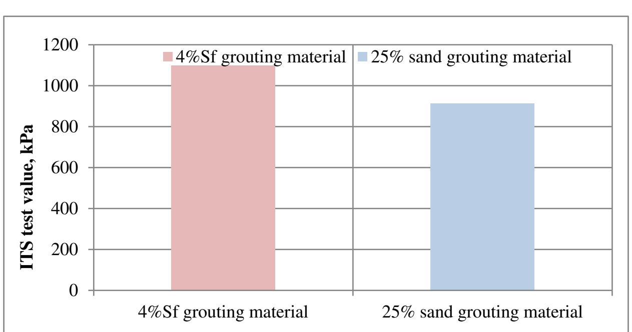

Figure 14: ITS test results conducted on samples at 28-day curing age.

5.3 Compressive strength

The specimens undergo axial compression testing in the absence of any form of lateral support. The term "specimen failure" is operationally defined as the highest load encountered by the specimen while undergoing compression, as specified in the ASTM D1074-17 standard. Table 8 displays the compressive strength values of two SFP combinations and the corresponding two GMs employed. The study revealed that GMs alone have much greater compressive strength compared to SFP, and this is consistent with the conclusions reached by Setyawan [32]. This suggests that incorporating GM into the asphalt mixture can enhance its overall strength. Despite the significant variation in the compressive strength between the mixture improved by SF and others using sand, the two SFP mixtures exhibit comparable compressive strength. This observation suggests that the vulnerable area in the SFP is located within the asphalt layer. These results are consistent with the findings of Wang and Hang [18] and differ from those of Yang [5], who showed an increase in the compressive strength of the SFP with an increase in the compressive strength of the GM. The reason for the difference in these conclusions may be due to the materials used in the production of SFP if the testing conditions are proven.

Table 8: Results of compressive strength

Mixture type	Compressive strength, MPa		
	1 day	7 days	28 days
*GM, 4% SF	24.3	32.7	48.1
GM, 25% sand	9.3	13	20.8
**CM, 4% SF	—	—	6.7
CM, 25% sand	—	—	6.3

*Grouting material.

**Composite material (here, it is SFP).

Figure 15: Samples after ITS test.

5.4 Wheel track test

The wheel track test is commonly employed for the assessment of rut depth in asphalt concrete mixtures which can be defined as a bowl-shaped depression in the wheel paths that develop gradually with the increasing number of load applications [33]. This testing method is increasingly favoured due to its ability to replicate actual traffic conditions closely [32], where the bituminous material performance is affected basically by the prevailing temperatures [34,35]. The samples for the rutting test were prepared as mentioned in Section 4. The test was performed according to BS EN12697-22:2003, which provides information about the rate of permanent deformation from moving of concentrated load, using a dial gauge or ruler to measure the permanent deformation of the specimen, as shown in Figure 15. The applied loaded wheel was 70 kg (158 pounds) at contact points and passed repetitively over the sample to be moved backwards and forward. The test temperature was 50°C, and the total distance of tire travel on the centre of the top surface of the specimen was 230 ± 10 mm. The loading frequency remains constant at 25 load cycles every 60 s. The maximum deformation was observed when the settling of the asphalt mixture reached a value of 20 mm or when the number of cycles reached 10,000 cycles, whichever occurred first [36]. The results showed a high resistance to rutting for the two SFP mixtures compared to the porous reference mixture, which had a high rutting value. The reason for this is due to the influence of the GM, which increases the stiffness of the mixture and gives it a hardness that resists this damage. Figures 16 and 17 show the test results for the tested samples.

It is also clear from the results that a slight difference exists between the final test result for the two mixtures of SFP, which amounted to 2.1 mm for the grouting material of SF (GMSF) mixture and 3.3 mm for the grouting material of sand (GMSN) mixture. The reason for this is that a material with high hardness supported the structure of the

Figure 16: Rutting test.

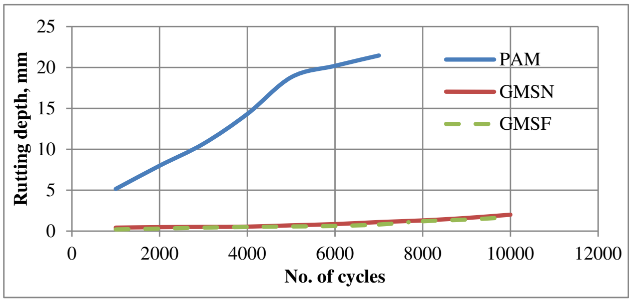

Figure 17: Wheel truck test result for 28-day curing age samples.

porous mixture. The value of the differential resistance of the two mixtures slightly affects the final test result. Yang [5] found that the results of the rutting test show that the SFP material mixed with the GM exhibits good high-temperature stability, and the dynamic stability increases with the increase in the strength of the GM.

6 Durability evaluation

Two tests were carried out to assess the durability of SFP: the first is the TSR test to evaluate the effect of this type on moisture, and the second is the Cantabro loss test to assess its vulnerability to ageing.

6.1 Moisture sensitivity (tensile strength ratio [TSR] test)

This test method covers the change in the diametrical tensile strength resulting from the effect of water saturation and accelerated water conditions with the freeze/thaw cycle of the compacted asphalt mixture. Traffic loading and climatic conditions may cause tensile stresses to develop within the pavement, and result in two types of cracks called fatigue cracking and thermal or shrinkage cracking. The standard method (AASHTO T283-14) [37] was used to evaluate the moisture susceptibility (TSR) of SFP samples. The TSR values for the two types of mixtures were extracted from the results of the ITS test for the two types of samples, conditioned and unconditioned, by using the following equation:

$$\mathrm{TSR} = \mathrm{Sw}/\mathrm{Sd} \times 100, \tag{4}$$

where TSR is the ITS ratio, % Sd is the average of ITS of dry unconditioned samples, kPa, and Sw is the average of ITS of wet conditioned samples, kPa.

The results presented in Figure 18 show that the TSR value of conditioned samples is lower than unconditioned samples, and this is due to the conditions that the sample is exposed to, such as humidity and heat. It is also clear from the results that the TSR value of the GMSF mixture is relatively more than that of GMSN. The approved specification requires a TSR value of more than 80%. The results obtained from the test are accepted with the required amount.

6.2 Cantabro loss test

The purpose of this test is to simulate mixture resistance to erosion (wear) ravelling and indirectly evaluate cohesion bonding and traffic abrasion effects. This test has been applied to determine the value of abrasion loss for the asphalt mixtures using the "Los Angeles Machine" Test Method (ASTMC131-14) and to expect the durability of OGFC pavements in the laboratory and during service life. The abrasion loss of specimens should not exceed 20% for unaged samples and 30% for the aged specimens. The results show that the Cantabro loss values of specimens that have been aged are greater than those of unaged specimens. This test was carried out on the Marshall sample for unaged and aged conditions according to ASTM D7064-13. Three samples were prepared for each asphalt content, as shown in Figure 19. Samples are weighed before and after the examination to calculate the loss value. The test results were calculated using the following equation and are presented in Figure 20:

$$P = \left(\frac{P_1 - P_2}{P_1}\right) \times 100, \tag{5}$$

where P is the Cantabro abrasion loss, %; P_1 is the initial weight of the sample, g; and P_2 is the final weight of the sample, g.

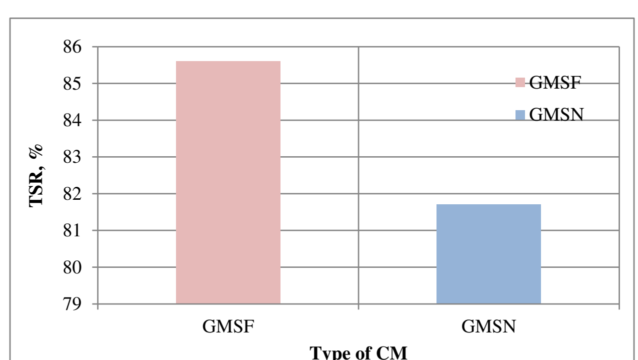

Figure 18: TSR values for two types of CMs at 28 days.

Figure 19: Sample for the Cantabro loss test.

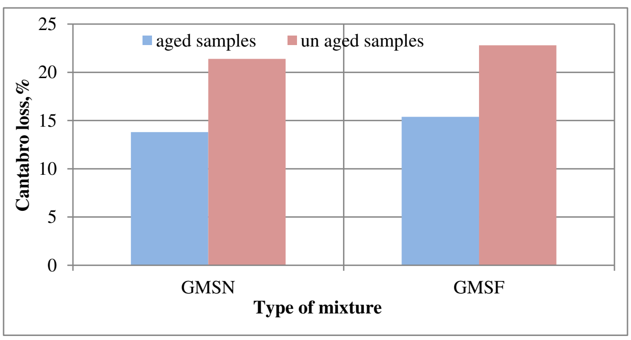

Figure 20: Cantabro loss test results for aged and unaged 28-day curing samples.

7 Conclusions

Based on the comprehensive analysis of the existing literature about SFP and its performance, as well as the subsequent laboratory experimentation and result analysis, it can be deduced that this material presents a feasible alternative for the advancement of high-performance pavement infrastructure. However, it is imperative to undertake endeavours aimed at establishing a standardized technique for the mixed design. The present study summarizes the key findings and conclusions:

1. Grouting a cement slurry with high fluidity into a porous, highly gradient asphalt mixture leads to a very large increase in the resistance of the porous mixture. The strength of the cement mixture is an important factor in the final performance of the semiflexible paving resulting from this process.

2. The homogeneity between the GMs is very important to achieve the required penetration of the PAM. The achievement of liquidity with the lack of homogeneity between the mixed GM may lead to the accumulation of the coarse material on the surface of the PAM as a result of the accuracy of the air spaces in it, causing the material to stop penetrating the porous layer.

3. The findings from the Marshall and rutting tests indicate that the incorporation of SFP material with the GM demonstrates favourable thermal stability at elevated temperatures. Additionally, it was observed that the Marshall stability of the mixture improves as the strength of the GM increases. In comparison to GMSN, with a strength of 20.8 MPa, GMSF, with a strength of 48.1 MPa, demonstrates a significant increase of 39.54% in Marshall stability after 28 days of curing. Furthermore, the comparative analysis revealed that the crumb rubber modified (CM) asphalt mixes exhibited superior resistance to rutting compared to conventional asphalt mixtures. This was observed using a wheel track rutting test, wherein the CM asphalt mixtures endured 10,000 wheel track cycles without exceeding a maximum rut depth of 2 mm.

4. The results of the ITS test showed a discrepancy between the two types of composite materials (CMs), and this is due to the difference in the strength of the GMs used, as the ITS value of the GMSF mixture increased by 14.91% compared with GMSN for the curing age of 28 days for unconditioned samples and by 20.22% for the conditioned samples for the same curing age.

5. The material remains flexible in addition to the hardness it gained from injecting the cement material in the presence of the asphalt material. This is evident in the results of the compressive strength test of the CM, which shows a large discrepancy between the compressive strength of the injection material for the same curing age.

6. The durability of two types of CM was measured by the Cantabro abrasion loss and tensile strength ratio. The results were acceptable and within the specification limits for the Cantabro loss test. With a variation for the two types of CMs, the GMSF mixture showed an increase in the value of Cantabro loss by 11.52% over the GMSN

mixture for ageing samples and 6.59% for non-ageing samples of 28 days of curing age.

8 Recommendations

In subsequent studies, it is recommended to conduct an on-site evaluation of a section of road using the semiflexible type of pavement and compare the efficiency of the process with the results achieved, as well as to study the microscopic structure of this type of pavement and work to increase the bonding strength between the asphalt for the porous mixture and the cement for the GM, which is considered one of the most important areas of strength for this type of pavement.

Funding information: This work was performed on the personal effort of the authors, and there was no funding effort from any side or organization.

Conflict of interest: The authors state no conflict of interest.

Data availability statement: Most datasets generated and analysed in this study are available in this manuscript. The other datasets are available on reasonable request from the corresponding author with the attached information.

References

[1] Bao L. French New Pavement Standard Structure Manual. Beijing, China: China Communications Press; 1987.
[2] Pelland RJ, Jonathan SG, Rajib BM. Selecting a rut-resistant hot mix asphalt for Boston-Logan International Airport. Airfield Pavements: Chall New Technol. 2004;390–408. doi: 10.1061/40711(141)26.
[3] Roffe JC. Salviacim–introducing the pavement. Paris, France: Jean Lefebvre Enterprise; 1989.
[4] Ahlrich RC, Gary LA. Construction and evaluation of resin modified pavement; Technical report GL 91–13, US army corps of engineers, Washington DC, 1991.
[5] Yang Q. Study of the effect of grouting material strength on semiflexible pavement material. Adv Mater Sci Eng. 2022;2022:5958896.
[6] Zhang J. Formulation and performance comparison of grouting materials for semiflexible pavement. Constr Build Mater. 2016;115:582–92.
[7] Ding QJ, Sun Z, Shen F, Huang SL. The performance analysis of semiflexible pavement by the volume parameter of matrix asphalt mixture. AMR. 2011;168–170:351–6.
[8] Zoorob S, Hassan K, Setyawan A. Cold mix, cold laid semiflexible grouted macadams, mix design and properties. In Performance of Bituminous and Hydraulic Materials in Pavements. London: Routledge; 2017. p. 105–12.
[9] Pei J, Cai J, Zou D, Zhang J, Li R, Chen X, et al. Design and performance validation of high-performance cement paste as a grouting material for semiflexible pavement. Constr Build Mater. 2016;126:206–17.
[10] Al-Qadi I, Gouru H, Weyers RE. Asphalt Portland cement concrete composite: laboratory evaluation. J Transp Eng. 1994;120(1):94–108.
[11] Hou S, Tao X, Kai H. Investigation into engineering properties and strength mechanism of grouted macadam composite materials. Int J Pavement Eng. 2016;17.10:878–86.
[12] Zhao W, Yang Q. Study on the applicability of asphalt concrete skeleton in the semiflexible pavement. Constr Build Mater. 2022;327:126923.
[13] Anderton GL. Engineering properties of resin modified pavement (RMP) for mechanistic design. US Army Corps of Engineers. Vicksburg, MS: Engineer Research and Development Center; 2000.
[14] Hao P, Cheng L, Lin L. Pavement performance Halls Ferry Road Vicksburg, MS 39180-6199 Final report of semiflexible pavement in laboratory. J Chang'an Univ. 2003;23(2):25–8.
[15] Zhao G, Huang C, Deng C. Performance of semiflexible pavement with different type. Highw Eng. 2017;4(1):199–201.
[16] Hassan KE, Setyawan A. Effect of cementitious grouts on the properties of semiflexible bituminous pavements. Proceedings of the 4th European Symposium on Performance of Bituminous and Hydraulic Materials in Pavements, Nottingham, UK, 11–12 April 2002; 2002.
[17] Zhou L. Temperature adaptability and failure mode analysis of semiflexible composite pavement. Ph.D. thesis. Chongqing, China: Chongqing Jiaotong; 2016.
[18] Wang K, Hong J. Hybrid concrete for advancing pavement performance. Iowa Highway Research Board; 2018. www.intrans.iastate.edu.
[19] Iraqi S. Portland cement The Central Organization for Iraqi Standard No. 5 and (in Arabic); 1984.
[20] Standard, A.J.C.C.-o.C., ed. West Conshohocken, PA, USA: ASTM International, C109/C109M-16a, Standard Test Method for Compressive Strength of Hydraulic Cement Mortars Cube Specimens; 2013.
[21] Hussein S, Al-Khafaji Z, Alfatlawi T, Abbood A. Improvement of permeable asphalt pavement by adding crumb rubber waste. Open Eng. 2022;12(1):1030–7. doi: 10.1515/eng-2022-0345
[22] ASTM D7064-13, "Standard Practice for Open-Graded Friction Course (OGFC) Mix Design", Annual book of ASTM standards. 2013.
[23] Husain NM, Mahmud HB, Karim MR, Hamid NBAA. Effects of aggregate gradations on properties of grouted Macadam composite pavement. In 2010 2nd International Conference on Chemical, Biological and Environmental Engineering, Cairo, Egypt, 2010, pp. 128–131, doi: 10.1109/ICBEE.2010.5653996.
[24] Ling TQ, Zhao ZJ, Xiong CH, Dong YY, Liu YY, Dong Q. The application of semiflexible pavement on heavy traffic roads. Int J Pavement Res Technol. 2009;2(5):211–7.
[25] Gawedzinski MJ, Gawedzinski MJ. Evaluation of Semiflexible (resin-coated) Pavement. Illinois Department of Transportation Bureau of Materials and Physical Research; Report No. I2008-01; 2008.
[26] ASTM C. 939. Standard test method for flow of grout for preplaced-aggregate concrete (flow cone method). Annu Book ASTM Stand. 2002;4.
[27] Koting S. Effects of using silica fume and polycarboxylate-type superplasticizer on physical properties of cementitious grout mixtures for semiflexible pavement surfacing. Sci World J. 2014(2014).
[28] ASTM A. D6927-15 Standard Test Method for Marshall Stability and Flow of Asphalt Mixtures. W.C., PA, USA: 2015.

[29] Standard AJAI. Standard test method for indirect tensile (IDT) strength of bituminous mixtures. West Conshohocken, PA: 2012.
[30] Solouki A, Piergiorgio T, Cesare S. Thermally treated waste silt as geopolymer grouting material and filler for semiflexible pavements. Infrastructures. 2022;7.8:99.
[31] Momtaz MO, Ahmed EAE-M, Zeinab SH. Assessing and improving the performance of grouted macadam. Am J Eng Appl Sci. 2020;13(2):153–64.
[32] Setyawan A. Asessing the compressive strength properties of semiflexible pavements. Proc Eng. 2013;54:863–74.
[33] Albayati A. A review of rutting in asphalt concrete pavement. Open Eng. 2023;13(1):20220463. doi: 10.1515/eng-2022-0463.
[34] Hilal M, Fattah M. A model for variation with time of flexiblepavement temperature. Open Eng. 2022;12(1):176–83. doi: 10.1515/eng-2022-0012.
[35] Sadiq N, Hilal MM, Fattah MY. Analysis of asphalt geogrid reinforced pavement rutting by finite element method. IOP Conf. Ser.: Earth Environ. Sci. 2022;961:012049.
[36] Hilal MM, Fattah MY. Evaluation of resilient modulus and rutting for warm asphalt mixtures: A local study in Iraq. Appl. Sci. 2022;12:12841. doi: 10.3390/app122412841.
[37] AASHTO T283-14. Standard method of test for resistance of compacted asphalt mixture to moisture-induced damage. American Association of State highway and Transportation Officials. Washington; D.C: 2014.